IEEE Access
Multidisciplinary | Rapid Review | Open Access Journal

Received July 21, 2019, accepted August 10, 2019, date of publication August 19, 2019, date of current version September 4, 2019.

Digital Object Identifier 10.1109/ACCESS.2019.2936321

Outage Performance of NOMA in Cooperative Cognitive Radio Networks With SWIPT

YUEHAO YU[1], ZHENG YANG[1], YI WU[1], JAMAL AHMED HUSSEIN[2], WEN-KANG JIA[1], AND ZHICHENG DONG[3]

[1]Fujian Provincial Engineering Technology Research Center of Photoelectric Sensing Application, Key Laboratory of OptoElectronic Science and Technology for Medicine of Ministry of Education, Fujian Normal University, Fuzhou 350007, China
[2]Ministry of Transportation and Communications—KRG, Sulaimaniyah 46001, Iraq
[3]School of Engineering, Tibet University, Lhasa 85000, China

Corresponding author: Zheng Yang (zyfjnu@163.com)

The work of Y. Yu, Z. Yang, Y. Wu, and W. Jia was supported in part by the National Natural Science Foundation of China under Grant U1805262, Grant 61701118, Grant 61571128, and Grant 61871131, and in part by the Natural Science Foundation of Fujian Province, China, under Grant 2018J05101. The work of Z. Dong was supported by the National Natural Science Foundation of China under Grant 61561046.

ABSTRACT This paper considers the application of non-orthogonal multiple access (NOMA) into cooperative cognitive radio (CR) networks with simultaneous wireless information and power transfer (SWIPT). For NOMA in cooperative CR networks with SWIPT, the cognitive relay harvests the transmission power from the secondary transmitter with power splitting scheme, while the fixed power allocation scheme is used for the NOMA protocol. The closed-form analytical expression of the overall outage probability for the proposed networks is derived, as well as its diversity order at high signal-to-noise ratio (SNR) region is investigated. Furthermore, compared to OMA in cooperative CR networks with SWIPT, the proposed scheme can always achieve the same diversity order, but lower overall outage performance. Compared with NOMA in cooperative CR networks using its own battery for transmission, the SWIPT NOMA in cooperative CR networks will lead to losing a little of the overall outage performance, but without losing the diversity order.

INDEX TERMS Non-orthogonal multiple access, cognitive radio network, decode-and-forward, simultaneous wireless information and power transfer, outage probability, diversity gain.

I. INTRODUCTION

Non-orthogonal multiple access (NOMA) has been regarded as an important enabling technology for the fifth generation (5G) wireless networks. This is due to the fact that NOMA can improve the spectrum efficiency of the overall system and provide better fairness in serving users [1]–[3]. In addition, it utilizes the orthogonal resource block more efficiently than within OMA scheme. The key concept of NOMA is that the scheme of the superposition coding is applied at the base station and the detection of the successive interference cancellation (SIC) is employed at the receivers. Recently, the downlink NOMA scheme has been proposed to the 3rd generation partnership project long-term evolution (3GPP-LTE) systems and the next generation network of the cellular communication [4], [5].

The associate editor coordinating the review of this manuscript and approving it for publication was Mohammad S. Khan.

The outage performance and ergodic capacity of the downlink and uplink NOMA scenario with fixed power allocation scheme have been studied in [6], [7]. Furthermore, a dynamic power allocation scheme for the uplink and downlink NOMA scenarios has been investigated in [8], which can always achieve better performance and fairness than those of OMA scenarios. Cooperative NOMA networks have been recognized as a crucial approach to further improve spectral efficiency, especially for users with poor channel condition [9]. According to different requirements of the users' quality of service (QoS), some two-stage relay selection strategies for the cooperative NOMA networks have been proposed in [10], [11]. Two studies [12], [13] have considered cooperative cognitive radio (CR) NOMA networks, and they have shown that the performance of the secondary receivers can be significantly improved compared to OMA in cooperative CR networks. In [14], the secondary user scheduling strategy for cooperative multicast cognitive radio NOMA systems

(MCR-NOMA) has been used to study the performance of the network.

In the traditional cooperative NOMA networks, the relays use their own batteries to forward the received messages from the source node, which will lead to improving the overhead. Fortunately, the technology of simultaneous wireless information and power transfer (SWIPT) can significantly reduce the energy consumption of the constrained network and enhance the lifetime of the battery [15]. Two energy harvesting schemes at the receiver nodes have been proposed in [16], namely; power splitting (PS) and time switching (TS). The authors in [17], have studied a wireless-powered uplink communication system with NOMA for one base station and multiple energy harvesting users. In their investigations, a greedy algorithm has been proposed for the time-sharing strategy to optimize the performance and user fairness of the wireless-power NOMA networks. In [18], the authors have considered cooperative NOMA networks with SWIPT, where the stronger user harvests energy from the base station to help the user with the poor condition in order to further enhance its throughput. In [19], the authors have proposed two types of NOMA power allocation schemes, the fixed power allocation and CR inspired power allocation for cooperative SWIPT NOMA networks, it has been shown that both schemes can significantly enhance the reliability of the network compared to the cooperative SWIPT OMA networks.

The main contributions of this paper are summarized as listed in the following:

- The SWIPT-aided cooperative CR NOMA networks is proposed, where the cognitive relay harvests the transmission power from the secondary transmitter with the PS scheme. By utilizing the decode-and-forward protocol at the cognitive relay that requires to decode the messages for two cognitive receivers and forward the encoding messages based on the NOMA scheme by using the harvested energy. As a result, the cognitive relay retransmits the encoded signals to the secondary receivers without consuming any energy from its own battery, which will prolong the battery life at the cognitive relay node.
- For SWIPT NOMA in cooperative CR networks, we consider overall outage probability as a performance criterion and derive its exact closed-form expression. Then, we investigate the diversity gain at the high-SNR regime. When the maximal interference tolerant level from the secondary transmitter and the cognitive relay to the primary receiver is proportional to the maximal transmission power at the secondary transmitter, the SWIPT NOMA/OMA in cooperative CR networks can achieve the same diversity gain, but the overall outage probability of the former is lower than that of the latter. In addition, compared to the NOMA in cooperative CR networks by using the battery of the cognitive relay to forward the messages, the SWIPT NOMA in cooperative CR networks will increase a little of the overall outage performance, but without losing any diversity gain.

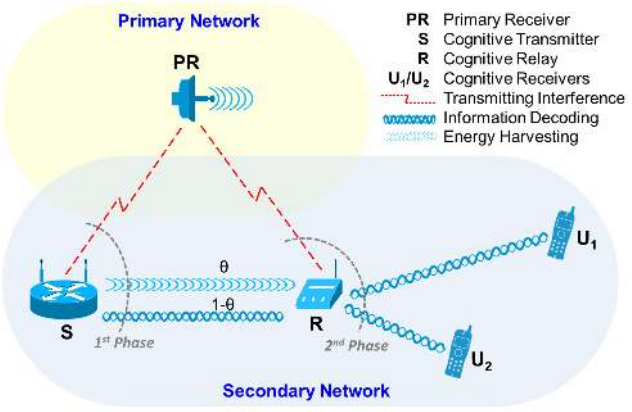

FIGURE 1. A cooperative CR NOMA network with SWIPT.

II. SYSTEM MODEL

We consider an underlay cooperative CR-NOMA network with SWIPT, as shown in Fig. 1. The system consists of a primary receiver (PR), a cognitive transmitter (S), two cognitive receivers (U_1 and U_2), and one cognitive relay (R), which harvests energy from the cognitive transmitter. It is assumed that the primary transmitter is located far away from the secondary network, thus the interference from the primary transmitter to the cognitive relay and the cognitive receivers can be omitted [12], [20]. Each of the nodes is equipped with a single antenna. The direct links between the cognitive transmitter and the cognitive receivers do not exist, which is due to the severe shadow fading. The cognitive relay R helps the cognitive transmitter to forward the intended signals to the cognitive receivers U_1 and U_2. All the channels are assumed to undergo quasi-static independent but not identically distributed (i.i.n.d) Rayleigh fading. The channel coefficients of the links $S \to PR$, $S \to R$, $R \to PR$, $R \to U1$, and $R \to U2$ are $h_{sp} \sim \mathcal{CN}(0, d_{sp}^{-\alpha/2})$, $h_{sr} \sim \mathcal{CN}(0, d_{sr}^{-\alpha/2})$, $h_{rp} \sim \mathcal{CN}(0, d_{rp}^{-\alpha/2})$, $h_{r1} \sim \mathcal{CN}(0, d_{r1}^{-\alpha/2})$, and $h_{r2} \sim \mathcal{CN}(0, d_{r2}^{-\alpha/2})$, respectively, where d_{sp}, d_{sr}, d_{rp}, d_{r1}, d_{r2} are the corresponding distances, and α is the path-loss factor. In addition, the NOMA protocol is applied to the SWIPT-based cooperative CR networks, where only the second order statistics is assumed to be available at the secondary transmitter and the cognitive relay to save the overhead of the channel estimation. The key concept of CR network is to opportunistically serve the secondary user on the condition that the primary user's QoS is guaranteed.

In the considered system, the transmission is performed within two phases, i.e., time slots. In the first time slot, the cognitive transmitter will broadcast the cognitive signal to the secondary relay node. To maintain the QoS at the primary receiver, the transmission power of the cognitive transmitter is constrained as follows:

$$P_s = \min\left\{P, \frac{I}{|h_{sp}|^2}\right\}, \tag{1}$$

where P stands for the maximum power of the secondary transmitter, and the interference at the primary receiver should not exceed the maximum tolerable level I.

Recall that the NOMA scheme is combined with the SWIPT-based CR network, thus, the cognitive transmitter S applies the superposition coding technique to combine two independent signals, i.e., $x = \sqrt{\alpha_1 P_s}x_1 + \sqrt{\alpha_2 P_s}x_2$, where x_1 and x_2 are intended messages to U_1 and U_2, respectively; α_i, $i = 1, 2$ is the power allocation factor for x_i, with $\alpha_1 > \alpha_2$ and $\alpha_1 + \alpha_2 = 1$. The power splitting (PS) protocol is applied at the cognitive relay node, with a splitting parameter $\omega(0 < \omega < 1)$ which is used to harvest the energy from the cognitive transmitter, and the remaining $(1-\omega)$ is utilized for information detection. Therefore, the received signal at the cognitive relay is given by:

$$y_R = \sqrt{(1-\omega)P_s}(\sqrt{\alpha_1}x_1 + \sqrt{\alpha_2}x_2)h_{sr} + \mathcal{N}_r, \tag{2}$$

where $\mathcal{N}_r$ represents the additive white Gaussian noise (AWGN) at the cognitive relay R, with $\mathcal{N}_r \sim \mathcal{CN}(0, \sigma^2)$.

According to the received signal in (2), the scheme of the SIC detection is used at the cognitive relay R to decode both signals x_1 and x_2. Without loss of generality, the cognitive relay R decodes the signal x_1, then extracts signal x_1 from the received signal, finally, it decodes signal x_2. Therefore, the corresponding signal-to-interference plus noise ratio (SINR), and signal-to-noise ratio (SNR) of the messages x_1 and x_2 at the cognitive relay R can be respectively expressed as:

$$\gamma^{\{x_1\}} = \frac{(1-\omega)|h_{sr}|^2\rho_s\alpha_1}{(1-\omega)|h_{sr}|^2\rho_s\alpha_2 + 1}, \tag{3}$$

and

$$\gamma^{\{x_2\}} = (1-\omega)|h_{sr}|^2\rho_s\alpha_2, \tag{4}$$

where $\rho_s = \frac{P_s}{\sigma^2}$ is the transmit SNR at the cognitive transmitter.

Based on (3) and (4), the messages x_1 and x_2 at the cognitive relay can be successfully decoded in the following cases: $R_R^1 = \frac{1}{2}\log_2(1+\gamma^{\{x_1\}}) \geq R_1^*$, $R_R^2 = \frac{1}{2}\log_2(1+\gamma^{\{x_2\}}) \geq R_2^*$, where R_1^* and R_2^* denote the targeted rate for U_1 and U_2, respectively. Note that the cognitive relay node needs to successfully decode both signals x_1 and x_2 from the received signal before it can harvest the energy. The main reason is that the superposition of the decoded signals x_1 and x_2 are forwarded by the cognitive relay to the cognitive receivers with the NOMA scheme in the second time slot. In addition, in order to ensure the cognitive relay can harvest the maximal energy from the cognitive transmitter, we impose two constraints, $R_R^1 = R_1^*$ and $R_R^2 = R_2^*$, which means the cognitive relay can correctly decode both x_1 and x_2 simultaneously, yet, the expense of the transmission power at the cognitive transmitter is minimal. Therefore,the expressions $R_R^1 = R_1^*$ and $R_R^2 = R_2^*$ can be written as follows:

$$\begin{cases} \frac{1}{2}\log_2(1+\gamma^{\{x_1\}}) = R_1^*; \\ \frac{1}{2}\log_2(1+\gamma^{\{x_2\}}) = R_2^*. \end{cases} \tag{5}$$

After some algebraic manipulations, and based on (3) and (4), formulas in (5) can be rewritten as:

$$\begin{cases} (1-\omega)\rho_s|h_{sr}|^2(1-2^{2R_1^*}\alpha_2) = 2^{2R_1^*} - 1; \\ (1-\omega)\rho_s|h_{sr}|^2 = 2^{2R_2^*} - 1. \end{cases} \tag{6}$$

Solving this binary linear equation, we can obtain the expression of the power allocation factor α_2 and the splitting parameter ω as follows:

$$\alpha_2 = \frac{2^{2R_2^*} - 1}{2^{2R_1^*+2R_2^*} - 1}, \tag{7}$$

and

$$\omega = \begin{cases} 1 - \dfrac{\varepsilon}{\rho_s|h_{sr}|^2}, & \text{if } \rho_s|h_{sr}|^2 > \varepsilon; \\ 0, & \text{otherwise}, \end{cases} \tag{8}$$

where $\varepsilon = 2^{2R_1^*+2R_2^*} - 1$, $0 < \alpha_2 < 1$, and $\omega < 1$. Note that when $\rho_s|h_{sr}|^2 < \varepsilon$, i.e., $\omega = 0$, means there is no energy to be harvested by the relay node in the received signal from the cognitive transmitter, and all received signals from the cognitive transmitter are used for information decoding.

Recall that the PS protocol is applied at the cognitive relay, thus the harvested energy by the cognitive relay can be given by [16]:

$$E_{R'} = \frac{1}{2}\eta\omega P_s|h_{sr}|^2, \tag{9}$$

where η represents the energy harvesting coefficient, with $0 < \eta < 1$. Note that the relatively small power harvested from the AWGN is neglected. Furthermore, the harvested energy at the cognitive relay is only used to forward the encoding information to the cognitive receivers, while the energy for the case of circuit consumption, etc., is not considered [18].

Therefore, the transmit power at the cognitive relay is given by:

$$P_{R'} = \eta\omega P_s|h_{sr}|^2. \tag{10}$$

According to (8), the $P_{R'}$ in (10) can be expressed as follows:

$$P_{R'} = \begin{cases} \eta(|h_{sr}|^2 P_s - \varepsilon\sigma^2), & \text{if } \rho_s|h_{sr}|^2 > \varepsilon; \\ 0, & \text{otherwise}. \end{cases} \tag{11}$$

Substituting (1) into (11), $P_{R'}$ can be rewritten as follows:

$$P_{R'} = \begin{cases} \eta\left(|h_{sr}|^2 P - \varepsilon\sigma^2\right), & \text{if } |h_{sr}|^2 > \dfrac{\varepsilon}{\rho}, |h_{sp}|^2 < \dfrac{I}{\rho\sigma^2}; \\ \eta\left(\dfrac{|h_{sr}|^2 I}{|h_{sp}|^2} - \varepsilon\sigma^2\right), & \text{if } \dfrac{|h_{sr}|^2 I}{|h_{sp}|^2\sigma^2} > \varepsilon, |h_{sp}|^2 > \dfrac{I}{\rho\sigma^2}; \\ 0, & \text{otherwise}. \end{cases} \tag{12}$$

In the second time slot, again, the interference to the primary user caused by the secondary relay in the like manner cannot exceed the thresholds I. Therefore, the power at the cognitive relay for forwarding the messages to the cognitive receivers can be expressed as follows:

$$P_R = \min\left\{P_{R'}, \frac{I}{|h_{rp}|^2}\right\}. \tag{13}$$

Recall that the second order statistics is available at the cognitive relay only, and assume that $d_{r1} > d_{r2}$. Based on NOMA scheme, the cognitive relay uses the superposition coding to mix the previously successfully decoded information x_1 and x_2, i.e., $x = \sqrt{\beta_1 P_R}x_1 + \sqrt{\beta_2 P_R}x_2$, and then retransmits it to the cognitive receivers U_i, $\{i = 1, 2\}$, where β_i denotes power allocation factor for U_i, $\beta_1 > \beta_2$ and $\beta_1 + \beta_2 = 1$. Therefore, the observation signal at U_i, $\{i = 1, 2\}$, is given by:

$$y_i = (\sqrt{\beta_1 P_R}x_1 + \sqrt{\beta_2 P_R}x_2)h_{ri} + \mathcal{N}_i, \tag{14}$$

where $\mathcal{N}_i$ indicates AWGN with $\mathcal{N}_i \sim \mathcal{CN}(0, \sigma^2)$.

According to NOMA protocol, the far user U_1 detecting its own message should regard the signal from the near user U_2 as the co-channel interference. Hence, the rate at the far user U_1 is given by:

$$R_1 = \frac{1}{2}\log_2\left(1 + \frac{\beta_1\rho_R|h_{r1}|^2}{\beta_2\rho_R|h_{r1}|^2 + 1}\right), \tag{15}$$

where $\rho_R = \frac{P_R}{\sigma^2}$.

Regarding the near user U_2, it requires to correctly decode the message x_1 before detecting its own message x_2 due to the fact that the detection of SIC is implemented at U_2. Hence, the achievable rate for U_2 to detect x_1 is given by:

$$R_{1\to 2} = \frac{1}{2}\log_2\left(1 + \frac{\beta_1\rho_R|h_{r2}|^2}{\beta_2\rho_R|h_{r2}|^2 + 1}\right). \tag{16}$$

When the condition $R_{1\to 2} \geq R_1^*$ is satisfied, i.e., the SIC can be successfully carried out at U_2 to remove the impact of signal x_1. Thus, the instantaneous rate for U_2 to detect x_2 can be calculated by:

$$R_2 = \frac{1}{2}\log_2\left(1 + \beta_2\rho_R|h_{r2}|^2\right). \tag{17}$$

III. OVERALL OUTAGE PROBABILITY FOR SWIPT-BASED NOMA IN COOPERATIVE CR NETWORKS

In this section, we focus on the fixed power allocation scheme at the secondary relay in the cooperative CR-NOMA networks with SWIPT, where more power is allocated to the far user than the near user to enhance the fairness among users. Furthermore, the overall outage probability of the entire network based on the fixed power allocation scheme is investigated. The overall complementary outage probability can be defined based on (13), (15), (16), and (17) as follows:

$$\overline{\mathrm{P}}_{out}^{F} = \Pr\left\{P_R > 0, R_1 \geq R_1^*, R_{1\to 2} \geq R_1^*, R_2 \geq R_2^*\right\}. \tag{18}$$

Note that $P_R > 0$ means the cognitive relay can successfully decode the messages which are intended for the cognitive receivers and it can also harvest the energy from the cognitive transmitter to forward the encoded messages. Furthermore, $R_1 \geq R_1^*$ means the far user U_1 can correctly decode its own message, while $R_1 \geq R_1^*$, and $R_{1\to 2} \geq R_1^*$ mean that the near user U_2 can successfully remove the message from the far user and its own message can also be successfully decoded, respectively.

According to the definition of overall complementary outage probability in (18), the analytical expression of the overall outage performance for the CR-NOMA networks with SWIPT is obtained in the following Theorem.

Theorem 1: The overall outage probability of SWIPT-based cooperative CR networks with NOMA scheme can be expressed as follows:

$$\begin{aligned}\mathrm{P}_{out}^{F} = {} & 1 - \left(1 - e^{-\frac{d_{sp}^{\alpha} I}{\rho\sigma^2}}\right)e^{-\frac{d_{sr}^{\alpha}\varepsilon}{\rho}}\left[\xi_1 K_1(\xi_1) - \xi_5 K_1(\xi_5)\right] \\ & - \int_{\frac{I}{\rho\sigma^2}}^{\infty} e^{-\frac{-d_{sr}^{\alpha}\varepsilon\sigma^2 y}{I}}\left[\xi_2 K_1(\xi_2) - \xi_3 K_1(\xi_3) + \xi_4 K_1(\xi_4)\right] \\ & \times d_{sp}^{\alpha} e^{-d_{sp}^{\alpha} y} dy - \frac{\left(1 - e^{-\frac{d_{sp}^{\alpha} I}{\rho\sigma^2}}\right)e^{-\frac{d_{sr}^{\alpha}\varepsilon}{\rho}} d_{rp}^{\alpha}}{(d_{r2}^{\alpha}\varphi'_{\max} + d_{r1}^{\alpha}\varphi'_1 + d_{rp}^{\alpha})}\left[\xi_5 K_1(\xi_5)\right],\end{aligned} \tag{19}$$

where

$$\begin{aligned}&\varepsilon_1 = 2^{2R_1^*} - 1, \quad \varepsilon_2 = 2^{2R_2^*} - 1, \\ &\beta_1 > \beta_2\varepsilon_1, \quad \varphi_1 = \frac{\varepsilon_1}{\eta(\beta_1 - \beta_2\varepsilon_1)}, \\ &\varphi_{\max} = \max\left\{\frac{\varepsilon_1}{\eta(\beta_1 - \beta_2\varepsilon_1)}, \frac{\varepsilon_2}{\eta\beta_2}\right\}, \quad \varphi'_1 = \frac{\eta\sigma^2}{I}\varphi_1, \\ &\varphi'_{\max} = \frac{\eta\sigma^2}{I}\varphi_{\max}, \quad \xi_1 = \sqrt{\frac{4d_{sr}^{\alpha}(d_{r2}^{\alpha}\varphi_{\max} + d_{r1}^{\alpha}\varphi_1)}{\rho}}, \\ &\xi_2 = \sqrt{\frac{4d_{sr}^{\alpha}(d_{r1}^{\alpha}\varphi_1\, y\sigma^2 + d_{r2}^{\alpha}\varphi_{\max} y\sigma^2)}{I}}, \\ &\xi_3 = \sqrt{\frac{4d_{sr}^{\alpha}(\eta d_{r1}^{\alpha}\varphi_1\, y\sigma^2 + \eta d_{r2}^{\alpha}\varphi_{\max} y\sigma^2 + d_{rp}^{\alpha} I y)}{\eta I}}, \\ &\xi_4 = \sqrt{\frac{4(d_{r2}^{\alpha}\varphi'_{\max} + d_{r1}^{\alpha}\varphi'_1 + d_{rp}^{\alpha})d_{sr}^{\alpha} y}{\eta d_{rp}^{\alpha}}}, \\ &\xi_5 = \sqrt{\frac{4\, I d_{sr}^{\alpha}(d_{r2}^{\alpha}\varphi_{\max'} + d_{r1}^{\alpha}\varphi'_1 + d_{rp}^{\alpha} I)}{\rho\eta\sigma^2}},\end{aligned}$$

and $K_1(.)$ is the first order modified Bessel function of the second kind [21].

Proof: See Appendix A.

Note that the developed analytical results of the overall outage performance in (19) can be used to evaluate the reliability for the NOMA SWIPT in CR networks through numerical simulation, compared to that of the OMA SWIPT in CR networks. On the other hand, it can be observed from (19) that the overall outage probability mainly depends on the parameters of the maximum cognitive transmitter power P and the maximum tolerable level I. In order to investigate

how the parameters of P and I affect the diversity gain, two Corollaries are studied in the following.

Corollary 1: Assume that I is proportional to ρ, i.e., $I = k\rho$. At high SNR range, i.e., $\rho \to \infty$, the overall outage probability P_{out}^{F} can be approximated as follows:

$$\mathrm{P}_{out}^{F} \approx \frac{\ln \rho}{\rho}. \tag{20}$$

Proof: See Appendix B.

Corollary 1 demonstrates that when $I = k\rho$ and $\rho \to \infty$, the overall outage probability for the NOMA SWIPT in CR networks with the fixed power allocation scheme can achieve a diversity gain of 1. On the other hand, Corollary 1 also concludes that although the cognitive relay without using its own battery and with partial channel information of the distances from the cognitive receivers, the diversity gain of the overall outage probability for NOMA SWIPT in CR networks will not be decreased.

Corollary 2: Assume that I is a constant, i.e., $I \neq k\rho$. When $\rho \to \infty$, the diversity gain of the overall outage probability P_{out}^{F} in (19) is zero.

Proof: When I is a constant, the approximated term B in (44) becomes a constant.

Corollary 2 shows that when I is independent of ρ, the overall outage performance only depends on I, although $\rho \to \infty$. This is because when I is a constant and $\rho \to \infty$, the transmit power of the cognitive transmitter P_s and the cognitive relay P_R in (1) and (13) should be rewritten as $P_s = \frac{I}{|h_{sp}|^2}$ and $P_R = \frac{I}{|h_{rp}|^2}$, respectively. Therefore, even at high SNR region, the approximated analytical results are only related to the maximal tolerance I, and the diversity gain reduces to zero.

IV. NUMERICAL RESULTS

In this section, we provide the Monte Carlo simulation results over 10^6 independent trials to verify the correctness of derived theoretical expressions of the overall outage performance for NOMA in CR networks with SWIPT. This relatively high number of trials makes the simulation results more precise and closer to the theoretical results. Meanwhile, the error bars has been added in Figs. 2 and 4 in order for the results to have better and more intuitive statistical significance.

Suppose that the path-loss factor $\alpha = 4$, the energy efficiency $\eta = 0.6$, the distances $d_{sr} = d_{sp} = d_{rp} = d_{r2} = 1\ m$, $d_{r1} = 3\ m$, the range of SNR $10 : 5 : 40\ dB$.

In Fig. 2, we assume that the power allocation ratio $\beta_1 = 0.8$, $\beta_2 = 0.2$, maximum tolerable level I is proportion to SNR $I = k\rho$, two different target rates $R_1^* = 0.5\ b/s/Hz$, $R_2^* = 1.0\ b/s/Hz$; and $R_1^* = 0.5\ b/s/Hz$, $R_2^* = 2.5\ b/s/Hz$. As shown in Fig. 2, the overall outage performance of the NOMA SWIPT in CR networks can always outperform OMA SWIPT in CR networks for a different target data rate of users. Especially, as the gap of the R_1^* and R_2^* increased, the overall outage performance of the proposed network can significantly improve compared to the tradition OMA in CR network with SWIPT. Furthermore, we can observe from the results in Fig. 2 that the developed analytical results in Theorem 1 are closed to the Monte Carlo simulations, which means the correctness of the analytical results of the overall outage probability in (19). In addition, Fig. 2 demonstrates that the overall outage probability can realize a diversity gain of one at high SNR region, which is consistent with the theoretical results in Corollary 1.

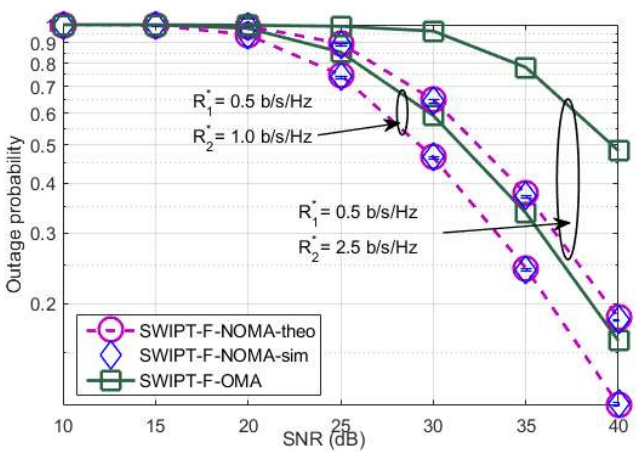

FIGURE 2. The effect of the different users' target data rates on the overall outage probability for the NOMA/OMA in cooperative CR networks with SWIPT, where $\beta_1 = 0.8$, $\beta_2 = 0.2$, and $I = k\rho$.

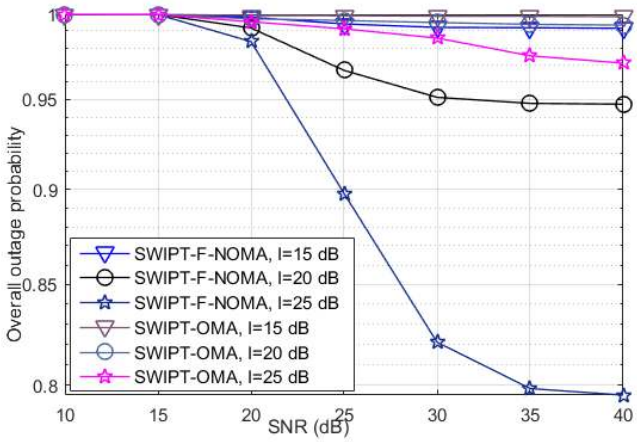

FIGURE 3. The impact of maximum tolerable level I on the overall outage performance in SWIPT NOMA/OMA in CR networks, where $\beta_1 = 0.8$, $\beta_2 = 0.2$.

In Fig. 3, we suppose $I \neq k\rho$, i.e., diverse constants 15, 20, 25 dB, the power allocation ratio $\beta_1 = 0.8$, $\beta_2 = 0.2$. Fig. 3 shows the overall outage probability versus the transmission SNR with the constant maximal tolerable level for the NOMA and OMA in CR networks with SWIPT. By observing Fig. 3, we can deduce the fact that the diversity gain of the overall outage probability for NOMA/OMA SWIPT in CR networks trends to zero at high SNR when the maximal interference level I does not yield a proportional variation with P, which is consistent with the analytical results in Corollary 2. However, we can still catch sight of the truth from Fig. 3 that NOMA in CR networks with SWIPT can

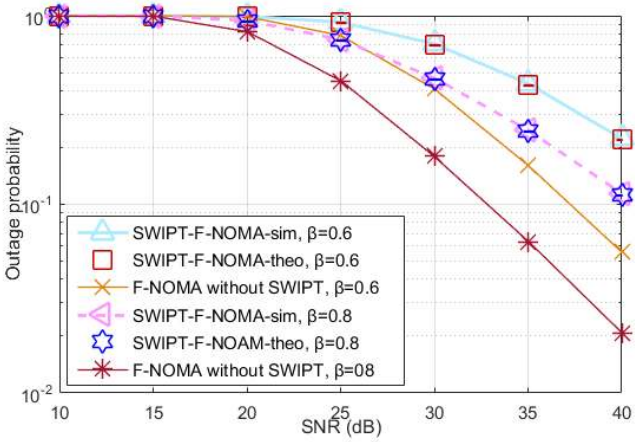

FIGURE 4. Overall outage probability comparison with/without SWIPT for NOMA in cooperative CR networks under different power allocation factors.

always surpass OMA in CR networks with SWIPT when I is a constant.

Fig. 4 shows the overall outage probability with/without SWIPT on NOMA with cooperative CR networks for different power allocation factors $\beta_1 = 0.6$, $\beta_1 = 0.8$. One can be seen from Fig. 4 that all lines are parallel at high SNR region, which means the application of SWIPT in cooperative CR NOMA networks will not lose the diversity gain. However, using SWIPT technique at the relay node will increase the overall outage probability, this is due to the fact that the transmission power of the cognitive relay is harvested from the secondary transmitter, and the conventional cooperative NOMA without SWIPT consuming its own battery to handle the relay transmission.

V. CONCLUSIONS

In this paper, we have derived the exact analytical expression of the overall outage probability for the NOMA in cooperative CR networks with SWIPT, and investigated its diversity gain at high SNR region. Both of the theoretical derivation and simulation results reveal that SWIPT NOMA in cooperative CR networks can achieve better overall outage performance than the OMA in cooperative CR networks with SWIPT. Furthermore, our theoretical results demonstrate that compared to the cooperative CR NOMA networks using its own battery for handling transmission, the application of SWIPT into cooperative CR NOMA networks does not decrease the diversity gain.

APPENDIX A
PROOF OF THEOREM 1

Based on (15), (16), (17) and (18), the overall complementary outage probability of the NOMA in CR networks with SWIPT can be represented as follows:

$$\overline{\mathrm{P}}_{out}^{F} = \Pr\left(\frac{\beta_1\rho_R|h_{r1}|^2}{\beta_2\rho_R|h_{r1}|^2+1} > \varepsilon_1, \frac{\beta_1\rho_R|h_{r2}|^2}{\beta_2\rho_R|h_{r2}|^2+1} > \varepsilon_1, \beta_2\rho_R|h_{r2}|^2 > \varepsilon_2, P_R > 0\right) \quad (21)$$

In consideration of (13), the ρ_R is a function of $P_{R'}$ and $\frac{I}{g_{rp}}$. According to the relationship between $P_{R'}$ and $\frac{I}{g_{rp}}$, the above probability $\overline{\mathrm{P}}_{out}$ can be further rewritten as follows:

$$\begin{aligned}
&\overline{\mathrm{P}}_{out}^{F} \\
&= \Pr\left(\frac{\beta_1\rho_R|h_{r1}|^2}{\beta_2\rho_{R'}|h_{r1}|^2+1} \geq \varepsilon_1, \frac{\beta_1\rho_{R'}|h_{r2}|^2}{\beta_2\rho_{R'}|h_{r2}|^2+1} \geq \varepsilon_1, |h_{sr}|^2 > \frac{\varepsilon}{\rho_s}, \rho_{R'} < \frac{I}{|h_{rp}|^2\sigma^2}, \beta_2\rho_{R'}|h_{r2}|^2 \geq \varepsilon_2\right)_{Q_1} \\
&+ \Pr\left(|h_{sr}|^2 > \frac{\varepsilon}{\rho_s}, \frac{\beta_2 I|h_{r2}|^2}{|h_{rp}|^2\sigma^2} \geq \varepsilon_2, \rho_{R'} > \frac{I}{|h_{rp}|^2\sigma^2}, \frac{\beta_1 I|h_{r1}|^2}{\beta_2 I|h_{r1}|^2+|h_{rp}|^2\sigma^2} \geq \varepsilon_1, \frac{\beta_1 I|h_{r2}|^2}{\beta_2 I|h_{r2}|^2+|h_{rp}|^2\sigma^2} \geq \varepsilon_1\right)_{Q_2}.
\end{aligned} \quad (22)$$

According to (1), the ρ_s is relate to P and $\frac{I}{|h_{sp}|^2}$. Based on the relationship between P and $\frac{I}{|h_{sp}|^2}$, the Q_1 and Q_2 in (22) can be further evaluated as follows:

$$\begin{aligned}
Q_1 =& \Pr\left(\frac{\beta_1\eta(\rho|h_{sr}|^2-\varepsilon)|h_{r1}|^2}{\beta_2\eta(\rho|h_{sr}|^2-\varepsilon)|h_{r1}|^2+1} \geq \varepsilon_1, |h_{sr}|^2 > \frac{\varepsilon}{\rho}, \eta(\rho|h_{sr}|^2-\varepsilon) < \frac{I}{|h_{rp}|^2\sigma^2}, \beta_2\eta(\rho|h_{sr}|^2-\varepsilon)|h_{r2}|^2 \geq \varepsilon_2, \right. \\
&\left. \frac{\beta_1\eta(\rho|h_{sr}|^2-\varepsilon)|h_{r2}|^2}{\beta_2\eta(\rho|h_{sr}|^2-\varepsilon)|h_{r2}|^2+1} \geq \varepsilon_1, \rho < \frac{I}{|h_{sp}|^2\sigma^2}\right)_{Q_{11}} \\
&+ \Pr\left(\frac{\beta_1\eta(\frac{|h_{sr}|^2 I}{|h_{sp}|^2\sigma^2}-\varepsilon)|h_{r1}|^2}{\beta_2\eta(\frac{|h_{sr}|^2 I}{|h_{sp}|^2\sigma^2}-\varepsilon)|h_{r1}|^2+1} \geq \varepsilon_1, \rho > \frac{I}{|h_{sp}|^2\sigma^2}, \beta_2\eta(\frac{|h_{sr}|^2 I}{|h_{sp}|^2\sigma^2}-\varepsilon)|h_{r2}|^2 \geq \varepsilon_2, \right. \\
&\left. \eta(\frac{|h_{sr}|^2 I}{|h_{sp}|^2\sigma^2}-\varepsilon) < \frac{I}{|h_{sp}|^2\sigma^2}, \frac{\beta_1\eta(\frac{|h_{sr}|^2 I}{|h_{sp}|^2\sigma^2}-\varepsilon)|h_{r2}|^2}{\beta_2\eta(\frac{|h_{sr}|^2 I}{|h_{sp}|^2\sigma^2}-\varepsilon)|h_{r2}|^2+1} \geq \varepsilon_1, |h_{sr}|^2 > \frac{\varepsilon\sigma^2|h_{sp}|^2}{I}\right)_{Q_{12}}.
\end{aligned} \quad (23)$$

$$\begin{aligned}
Q_2 =& \Pr\left(\frac{|h_{r2}|^2}{|h_{rp}|^2} \geq \frac{\varepsilon_1\sigma^2}{I(\beta_1-\beta_2\varepsilon_1)}, \frac{|h_{r1}|^2}{|h_{rp}|^2} \geq \frac{\varepsilon_1\sigma^2}{I(\beta_1-\beta_2\varepsilon_1)}, \eta(\rho|h_{sr}|^2-\varepsilon) > \frac{I}{|h_{rp}|^2\sigma^2}, |h_{sr}|^2 > \frac{\varepsilon}{\rho}, |h_{sp}|^2 < \frac{I}{\rho\sigma^2}, \right. \\
&\left. \frac{|h_{r2}|^2}{|h_{rp}|^2} \geq \frac{\varepsilon_2\sigma^2}{\beta_2 I}\right)_{Q_{21}} + \Pr\left(\frac{|h_{r2}|^2}{|h_{rp}|^2} \geq \frac{\varepsilon_1\sigma^2}{I(\beta_1-\beta_2\varepsilon_1)}, \frac{|h_{r2}|^2}{|h_{rp}|^2} \geq \frac{\varepsilon_2\sigma^2}{\beta_2 I}, \frac{|h_{r1}|^2}{|h_{rp}|^2} \geq \frac{\varepsilon_1\sigma^2}{I(\beta_1-\beta_2\varepsilon_1)}, |h_{sp}|^2 > \frac{I}{\rho\sigma^2}, \right. \\
&\left. |h_{sr}|^2 > \frac{\varepsilon\sigma^2|h_{sp}|^2}{I}, |h_{rp}|^2 > \frac{I|h_{sp}|^2}{\eta(I|h_{sr}|^2-\varepsilon|h_{sp}|^2\sigma^2)}\right)_{Q_{22}}.
\end{aligned} \quad (24)$$

Note that the channel fading gains of all links in the entire system model are obey exponential distribution with

different expectations. Therefore, the probability density function (PDF) and cumulative distribution function (CDF) of the channel fading gains $* \in \{sr, sp, rp, r_1, r_2\}$ are respectively given by

$$f_{|h_*|^2}(x) = d_*^{\alpha} e^{-d_*^{\alpha} x}, \quad x > 0, \tag{25}$$

and

$$F_{|h_*|^2}(x) = 1 - e^{-d_*^{\alpha} x}, \quad x > 0. \tag{26}$$

Let $x = g_{sr}$, $y = g_{sp}$, $z = g_{rp}$, $u = g_{r1}$, $v = g_{r2}$, and based on (25) and (26), Q_{11} in (23), and Q_{21} in (24) can be respectively evaluated as follows:

$$\begin{aligned} Q_{11} &= \Pr\left(|h_{r1}|^2 \geq \frac{\varphi_1}{\rho|h_{sr}|^2 - \varepsilon}, |h_{rp}|^2 < \frac{I}{\eta\sigma^2(\rho|h_{sr}|^2 - \varepsilon)}\right. \\ &\quad \left. |h_{r1}|^2 \geq \frac{\varphi_{\max}}{\rho|h_{sr}|^2 - \varepsilon}, |h_{sr}|^2 > \frac{\varepsilon}{\rho}, |h_{sp}|^2 < \frac{I}{\rho\sigma^2}, \right) \\ &= \int_0^{\frac{I}{\rho\sigma^2}} \int_{\frac{\varepsilon}{\rho}}^{\infty} \int_0^{\frac{I}{\eta\sigma^2(\rho x - \varepsilon)}} \int_{\frac{\varphi_1}{\rho x - \varepsilon}}^{\infty} \int_{\frac{\varphi_{max}}{\rho x - \varepsilon}}^{\infty} d_{r2}^{\alpha} d_{r1}^{\alpha} d_{rp}^{\alpha} d_{sr}^{\alpha} d_{sp}^{\alpha} \\ &\quad \times e^{-d_{r2}^{\alpha} v} dv e^{-d_{r1}^{\alpha} u} du e^{-d_{rp}^{\alpha} z} dz e^{-d_{sr}^{\alpha} x} dx e^{-d_{sp}^{\alpha} y} dy \\ &= \left(1 - e^{-\frac{d_{sp}^{\alpha} I}{\rho\sigma^2}}\right) \int_{\frac{\varepsilon}{\rho}}^{\infty} \left(1 - e^{-\frac{d_{rp}^{\alpha} I}{\eta\sigma^2(\rho x - \varepsilon)}}\right) e^{-\frac{d_{r2}^{\alpha}\varphi_{max} + d_{r1}^{\alpha}\varphi_1}{\rho x - \varepsilon}} \\ &\quad \times d_{sr}^{\alpha} e^{-d_{sr}^{\alpha} x} dx. \end{aligned} \tag{27}$$

$$\begin{aligned} Q_{21} &= \Pr\left(|h_{r1}|^2 \geq \varphi_1' |h_{rp}|^2, |h_{rp}|^2 > \frac{I}{\eta\sigma^2(\rho|h_{sr}|^2 - \varepsilon)}, \right. \\ &\quad \left. |h_{r2}|^2 \geq \varphi_{max}' |h_{rp}|^2, |h_{sr}|^2 > \frac{\varepsilon}{\rho}, |h_{sp}|^2 < \frac{I}{\rho\sigma^2} \right) \\ &= \int_0^{\frac{I}{\rho\sigma^2}} \int_{\frac{\varepsilon}{\rho}}^{\infty} \int_{\frac{I}{\eta\sigma^2(\rho x - \varepsilon)}}^{\infty} \int_{\varphi_1' z}^{\infty} \int_{\varphi_{max}' z}^{\infty} d_{r2}^{\alpha} d_{r1}^{\alpha} d_{rp}^{\alpha} d_{sr}^{\alpha} d_{sp}^{\alpha} \\ &\quad \times e^{-d_{r2}^{\alpha} v} dv e^{-d_{r1}^{\alpha} u} du e^{-d_{rp}^{\alpha} z} dz e^{-d_{sr}^{\alpha} x} dx e^{-d_{sp}^{\alpha} y} dy \\ &= \frac{\left(1 - e^{-\frac{d_{sp}^{\alpha} I}{\rho\sigma^2}}\right) d_{rp}^{\alpha}}{d_{r2}^{\alpha}\varphi_{max}' + d_{r1}^{\alpha}\varphi_1' + d_{rp}^{\alpha}} \int_{\frac{\varepsilon}{\rho}}^{\infty} e^{-\frac{(d_{r2}^{\alpha}\varphi_{max}' + d_{r1}^{\alpha}\varphi_1' + d_{rp}^{\alpha})I}{\eta\sigma^2(\rho x - \varepsilon)}} \\ &\quad \times d_{sr}^{\alpha} e^{-d_{sr}^{\alpha} x} dx. \end{aligned} \tag{28}$$

Let $t = \rho x - \varepsilon$, Q_{11} in (27), and Q_{21} in (28) can be rewritten as follows:

$$\begin{aligned} Q_{11} &= \left(1 - e^{-\frac{d_{sp}^{\alpha} I}{\rho\sigma^2}}\right) \frac{1}{\rho} \int_0^{\infty} \left(1 - e^{-\frac{d_{rp}^{\alpha} I}{\eta\sigma^2 t}}\right) e^{-\frac{d_{r2}^{\alpha}\varphi_{max} + d_{r1}^{\alpha}\varphi_1}{t}} \\ &\quad \times e^{-\frac{d_{sr}^{\alpha}(t+\varepsilon)}{\rho}} d(d_{sr}^{\alpha} t). \end{aligned} \tag{29}$$

$$\begin{aligned} Q_{21} &= \frac{\left(1 - e^{-\frac{d_{sp}^{\alpha} I}{\rho\sigma^2}}\right) d_{rp}^{\alpha}}{(d_{r2}^{\alpha}\varphi_{max}' + d_{r1}^{\alpha}\varphi_1' + d_{rp}^{\alpha})\rho} \int_0^{\infty} e^{-\frac{d_{sr}^{\alpha}(t+\varepsilon)}{\rho}} \\ &\quad \times e^{-\frac{(d_{r2}^{\alpha}\varphi_{max}' + d_{r1}^{\alpha}\varphi_1' + d_{rp}^{\alpha})I}{\eta\sigma^2 t}} d(d_{sr}^{\alpha} t). \end{aligned} \tag{30}$$

Applying the formula $\int_0^{\infty} e^{-\frac{\beta}{4x} - \gamma x} = \sqrt{\frac{\beta}{\gamma}} K_1(\sqrt{\beta\gamma})$ in [21], the above expressions of Q_{11} and Q_{21} can be derived as follows:

$$\begin{aligned} Q_{11} &= \left(1 - e^{-\frac{d_{sp}^{\alpha} I}{\rho\sigma^2}}\right) e^{-\frac{d_{sr}^{\alpha}\varepsilon}{\rho}} \left[\xi_1 K_1(\xi_1) - \xi_5 K_1(\xi_5)\right] \\ Q_{21} &= \frac{\left(1 - e^{-\frac{d_{sp}^{\alpha} I}{\rho\sigma^2}}\right) \times e^{-\frac{d_{sp}^{\alpha}\varepsilon}{\rho}} d_{rp}^{\alpha}}{(d_{r2}^{\alpha}\varphi_{max}' + d_{r1}^{\alpha}\varphi_1' + d_{rp}^{\alpha})} \left[\xi_5 K_1(\xi_5)\right], \end{aligned} \tag{31}$$

Following the similar processes in the proof of (23) and (24), Q_{12} in (23) and Q_{22} in (24) can be further reformulated as follows:

$$\begin{aligned} Q_{12} &= \Pr\left(|h_{r1}|^2 \geq \frac{\varphi_1 |h_{sp}|^2 \sigma^2}{|h_{sr}|^2 I - \varepsilon|h_{sp}|^2\sigma^2}, \frac{|h_{sr}|^2}{|h_{sp}|^2} > \frac{\varepsilon\sigma^2}{I}, \right. \\ &\quad |h_{r2}|^2 \geq \frac{\varphi_{\max}|h_{sp}|^2\sigma^2}{|h_{sr}|^2 I - \varepsilon|h_{sp}|^2\sigma^2}, |h_{sp}|^2 > \frac{I}{\rho\sigma^2}, \\ &\quad \left. |h_{rp}|^2 < \frac{I|h_{sp}|^2\sigma^2}{\eta\sigma^2(|h_{sr}|^2 I - \varepsilon|h_{sp}|^2\sigma^2)} \right) \\ &= \int_{\frac{I}{\rho\sigma^2}}^{\infty} \int_{\frac{\varepsilon\sigma^2 y}{I}}^{\infty} [1 - e^{-\frac{d_{rp}^{\alpha} I y}{\eta(xI - \varepsilon\sigma^2 y)}}] e^{-\frac{d_{r1}^{\alpha}\varphi_1 \, y\sigma^2 + d_{r2}^{\alpha}\varphi_{\max} y\sigma^2}{Ix - \varepsilon\sigma^2 y}} \\ &\quad \times d_{sr}^{\alpha} e^{-d_{sr}^{\alpha} x} dx d_{sp}^{\alpha} e^{-d_{sp}^{\alpha} y} dy. \end{aligned} \tag{32}$$

$$\begin{aligned} Q_{22} &= \Pr\left(|h_{sr}|^2 > \frac{\varepsilon\sigma^2|h_{sp}|^2}{I}, |h_2|^2 \geq \varphi_{max}' |h_{rp}|^2, \right. \\ &\quad |h_{sp}|^2 > \frac{I}{\rho\sigma^2}, |h_{rp}|^2 > \frac{I|h_{sp}|^2}{\eta(|h_{sr}|^2 I - \varepsilon|h_{sp}|^2\sigma^2)}, \\ &\quad \left. |h_{r1}|^2 \geq \varphi_1' |h_{rp}|^2 \right) \\ &= \int_{\frac{I}{\rho\sigma^2}}^{\infty} \left[\int_{\frac{\varepsilon\sigma^2 y}{I}}^{\infty} e^{-\frac{Iy(d_{r2}^{\alpha}\varphi_{\max}' + d_{r1}^{\alpha}\varphi_1' + d_{rp}^{\alpha})}{d_{rp}^{\alpha}\eta(xI - \varepsilon\sigma^2 y)} - d_{sr}^{\alpha} x} d_{sr}^{\alpha} dx \right] \\ &\quad \times d_{sp}^{\alpha} e^{-d_{sp}^{\alpha} y} dy. \end{aligned} \tag{33}$$

Let $t = xI - \varepsilon\sigma^2 y$, Q_{12} in (32) and Q_{22} in (33) can be evaluated as follows:

$$\begin{aligned} Q_{12} &= \int_{\frac{I}{\rho\sigma^2}}^{\infty} \frac{e^{-\frac{-d_{sr}^{\alpha}\varepsilon\sigma^2 y}{I}}}{I} \left[\int_0^{\infty} (e^{-\frac{4d_{sr}^{\alpha}(d_{r1}^{\alpha}\varphi_1 y\sigma^2 + d_{r2}^{\alpha}\varphi_{\max} y\sigma^2)}{4d_{sr}^{\alpha} t}} \right. \\ &\quad \left. - e^{-\frac{4d_{sr}^{\alpha}(\eta d_{r1}^{\alpha}\varphi_1 y\sigma^2 + \eta d_{r2}^{\alpha}\varphi_{\max} y\sigma^2 + d_{rp}^{\alpha} I y)}{4\eta d_{sr}^{\alpha} t}}) e^{-\frac{d_{sr}^{\alpha} t}{I}} d(d_{sr}^{\alpha} t) \right] \\ &\quad \times d_{sp}^{\alpha} e^{-d_{sp}^{\alpha} y} dy \\ &= \int_{\frac{I}{\rho\sigma^2}}^{\infty} e^{-\frac{-d_{sr}^{\alpha}\varepsilon\sigma^2 y}{I}} \left[\xi_2 K_1(\xi_2) - \xi_3 K_1(\xi_3)\right] d_{sp}^{\alpha} e^{-d_{sp}^{\alpha} y} dy, \end{aligned} \tag{34}$$

$$\begin{aligned} Q_{22} &= \int_{\frac{I}{\rho\sigma^2}}^{\infty} \frac{e^{-\frac{d_{sr}^{\alpha}\varepsilon\sigma^2 y}{I}}}{I} \int_0^{\infty} e^{-\frac{(d_{r2}^{\alpha}\varphi_{\max}' + d_{r1}^{\alpha}\varphi_1' + d_{rp}^{\alpha})Iy 4 d_{sr}^{\alpha}}{\eta d_{rp}^{\alpha} 4 d_{sr}^{\alpha} t} - \frac{d_{sr}^{\alpha} t}{I}} \\ &\quad \times d(d_{sr}^{\alpha} t) d_{sp}^{\alpha} e^{-d_{sp}^{\alpha} y} dy \\ &= \int_{\frac{I}{\rho\sigma^2}}^{\infty} e^{-\frac{d_{sr}^{\alpha}\varepsilon\sigma^2 y}{I}} \left[\xi_4 K_1(\xi_4)\right] d_{sp}^{\alpha} e^{-d_{sp}^{\alpha} y} dy, \end{aligned} \tag{35}$$

Combining (31), (34) and (35), the Theorem 1 is completely proved.

APPENDIX B
PROOF OF COROLLARY 1

The overall outage probability in (19) can be divided into three parts as follows:

$$\begin{aligned}\overline{P}_{out}^{F} &= \underbrace{\left(1-e^{-\frac{d_{sp}^{\alpha}I}{\rho\sigma^2}}\right)e^{-\frac{d_{sr}^{\alpha}\varepsilon}{\rho}}\xi_1K_1(\xi_1)}_{A}+\underbrace{\left(1-e^{-\frac{d_{sp}^{\alpha}I}{\rho\sigma^2}}\right)e^{-\frac{d_{sr}^{\alpha}\varepsilon}{\rho}}}_{B}\\ &\times\underbrace{\left(\frac{1}{1+\frac{d_{r2}^{\alpha}\eta\sigma^2}{d_{rp}^{\alpha}I}\varphi_{\max}+\frac{d_{r1}^{\alpha}\eta\sigma^2}{d_{rp}^{\alpha}I}\varphi_1}-1\right)\xi_5K_1(\xi_5)}_{B}+\underbrace{\int_{\frac{I}{\rho\sigma^2}}^{\infty}d_{sp}^{\alpha}}_{C}\\ &\underbrace{\times e^{-\frac{d_{sr}^{\alpha}\varepsilon\sigma^2y}{I}-d_{sp}^{\alpha}y}\left[\xi_2K_1(\xi_2)+\xi_4K_1(\xi_4)-\xi_3K_1(\xi_3)\right]dy}_{C}.\end{aligned} \tag{36}$$

For $\rho\to\infty$, and $I=k\rho$, the approximation of the A, B, and C in (36) will be evaluated in the following.

A. THE APPROXIMATION OF A

When $x\to 0$, the Bessel function $xK_1(x)$ can be approximated by series [21]:

$$\begin{aligned}xK_1(x) &= 1+\sum_{k=0}^{\infty}\frac{(\frac{x}{2})^{2k+1}x}{k!\Gamma(k+2)}(\ln\frac{x}{2}+C)-\frac{1}{2}\sum_{l=0}^{\infty}\frac{(\frac{x}{2})^{2l+1}x}{l!(n+l)!}\\ &\times\Big(\sum_{k=1}^{l}\frac{1}{k}+\sum_{k=1}^{l+1}\frac{1}{k}\Big)\approx 1+\frac{x^2}{2}\ln\frac{x}{2}.\end{aligned} \tag{37}$$

When $x\to 0$, the exponential function can be approximated as follows:

$$e^{-x}\approx 1-x. \tag{38}$$

When $\rho\to\infty$, based on (37) and (38), and let $\pi_1=\frac{d_{sr}^{\alpha}(d_{r2}^{\alpha}\varphi_{\max}+d_{r1}^{\alpha}\varphi_1)}{\rho}$, we have

$$\xi_1K_1(\xi_1)\approx 1+\pi_1\ln\pi_1, \tag{39}$$

and

$$e^{-\frac{d_{sr}^{\alpha}\varepsilon}{\rho}}\approx 1-\frac{d_{sr}^{\alpha}\varepsilon}{\rho}. \tag{40}$$

Substituting (39) and (40) into the first term A in (36), the term A can be approximated as follows:

$$A\approx 1-\frac{d_{sr}^{\alpha}\varepsilon}{\rho}-e^{-\frac{kd_{sp}^{\alpha}}{\sigma^2}}\left(1-\frac{d_{sr}^{\alpha}\varepsilon}{\rho}\right)-\left(1-e^{-\frac{kd_{sp}^{\alpha}}{\sigma^2}}\right)\pi_1\ln\pi_1. \tag{41}$$

B. THE APPROXIMATION OF B

When $\rho\to\infty$, $I=k\rho$, and based on (19), the ξ_5 in B in (36) can be approximated as follows:

$$\begin{aligned}\xi_5 &= \sqrt{\frac{4d_{sr}^{\alpha}(d_{r2}^{\alpha}\varphi_{\max}+d_{r1}^{\alpha}\varphi_1)}{\rho}+\frac{4d_{sr}^{\alpha}d_{rp}^{\alpha}k}{\eta\sigma^2}}\\ &\approx\sqrt{\frac{4d_{sr}^{\alpha}d_{rp}^{\alpha}k}{\eta\sigma^2}}.\end{aligned} \tag{42}$$

On the basis of formula of expanded Taylor series $\frac{1}{1+x}=\sum_{n=0}^{\infty}(-1)^nx^n$, we have

$$\frac{1}{1+\frac{d_{r2}^{\alpha}\eta\sigma^2}{d_{rp}^{\alpha}I}\varphi_{\max}+\frac{d_{r1}^{\alpha}\eta\sigma^2}{d_{rp}^{\alpha}I}\varphi_1}\approx 1-\frac{d_{r2}^{\alpha}\eta\sigma^2}{d_{rp}^{\alpha}I}\varphi_{\max}-\frac{d_{r1}^{\alpha}\eta\sigma^2}{d_{rp}^{\alpha}I}\varphi_1. \tag{43}$$

Substituting (40), (42), and (43) into the second term B in (36), we can approximate the term B as follows:

$$\begin{aligned}B &\approx\left(1-e^{-\frac{kd_{sp}^{\alpha}}{\sigma^2}}\right)\left[-\frac{d_{r2}^{\alpha}\varphi_{\max}\eta\sigma^2+d_{r1}^{\alpha}\varphi_1\eta\sigma^2}{d_{rp}^{\alpha}I}\right]\\ &\times\sqrt{\frac{4d_{sr}^{\alpha}d_{rp}^{\alpha}k}{\eta\sigma^2}}K_1\left(\sqrt{\frac{4d_{sr}^{\alpha}d_{rp}^{\alpha}k}{\eta\sigma^2}}\right)\\ &\approx-\frac{C_2}{I},\end{aligned} \tag{44}$$

where

$$\begin{aligned}C_2 &= (1-e^{-\frac{kd_{sp}^{\alpha}}{\sigma^2}})(\frac{d_{r2}^{\alpha}\varphi_{\max}\eta\sigma^2+d_{r1}^{\alpha}\varphi_1\eta\sigma^2}{d_{rp}^{\alpha}})\\ &\times(\sqrt{\frac{4d_{sr}^{\alpha}d_{rp}^{\alpha}k}{\eta\sigma^2}}K_1(\sqrt{\frac{4d_{sr}^{\alpha}d_{rp}^{\alpha}k}{\eta\sigma^2}}))\end{aligned}$$

is a constant, independent of ρ or I.

C. THE APPROXIMATION OF C

Based on (37), $\xi_2K_1(\xi_2)$, $\xi_3K_1(\xi_3)$ and $\xi_4K_1(\xi_4)$ in the third term C in (36) can be expanded in the series as follows:

$$\begin{aligned}\xi_2K_1(\xi_2) &= 1+\sum_{k=0}^{\infty}\frac{(\frac{\xi_2}{2})^{2k+1}\xi_2}{k!\Gamma(k+2)}(\ln\frac{\xi_2}{2}+C)\\ &-\frac{1}{2}\sum_{l=0}^{\infty}\frac{(\frac{\xi_2}{2})^{2l+1}\xi_2}{l!(n+l)!}(\sum_{k=1}^{l}\frac{1}{k}+\sum_{k=1}^{l+1}\frac{1}{k}).\end{aligned} \tag{45}$$

Note that ξ_2, ξ_3, and ξ_4 contain the variable y, while the series of the second order Bessel function mainly contain the term of 1, $(\xi_2)^m\ln(\frac{\xi_2}{2})$, and $(\xi_2)^m$. Therefore, the $\xi_2K_1(\xi_2)$ in (45) can be approximated as follows:

$$\xi_2K_1(\xi_2)\approx 1+(\xi_2)^m\ln(\frac{\xi_2}{2})-(\xi_2)^m. \tag{46}$$

Based on (46), the third part C can be rewritten as follows:

$$\begin{aligned}C &\approx d_{sp}^{\alpha}\int_{\frac{I}{\rho\sigma^2}}^{\infty}e^{-(\frac{d_{sr}^{\alpha}\varepsilon\sigma^2+d_{sp}^{\alpha}I)y}{I}}[1+(\xi_2)^m\ln(\frac{\xi_2}{2})-(\xi_2)^m\\ &+(\xi_4)^m\ln(\frac{\xi_4}{2})-(\xi_4)^m-(\xi_3)^m\ln(\frac{\xi_3}{2})+(\xi_3)^m]dy.\end{aligned} \tag{47}$$

The first integral in (47) can be evaluated as follows:

$$\begin{aligned}C_1 &= d_{sp}^{\alpha}\int_{\frac{I}{\rho\sigma^2}}^{\infty}e^{-(\frac{d_{sr}^{\alpha}\varepsilon\sigma^2+d_{sp}^{\alpha}I)}{I}y}dy\\ &=\frac{d_{sp}^{\alpha}I}{d_{sr}^{\alpha}\varepsilon\sigma^2+d_{sp}^{\alpha}I}e^{-\frac{d_{sr}^{\alpha}\varepsilon\sigma^2+d_{sp}^{\alpha}I}{\rho\sigma^2}}\\ &\approx e^{-\frac{kd_{sp}^{\alpha}}{\sigma^2}}(1-\frac{d_{sr}^{\alpha}\varepsilon}{\rho}).\end{aligned} \tag{48}$$

Note that (47) contains two different variables y^m and $y^m \ln y$ in the integral, we can make the following definition:

$$D_3 = d_{sp}^{\alpha} \int_{\frac{I}{\rho\sigma^2}}^{\infty} e^{-(\frac{d_{sr}^{\alpha}\varepsilon\sigma^2 + d_{sp}^{\alpha} I}{I})y} y^m dy,$$
$$D_4 = d_{sp}^{\alpha} \int_{\frac{I}{\rho\sigma^2}}^{\infty} e^{-(\frac{d_{sr}^{\alpha}\varepsilon\sigma^2 + d_{sp}^{\alpha} I}{I})y} y^m \ln(y) dy. \quad (49)$$

Using the definition of the upper incomplete gamma function $\Gamma(s, x) = \int_x^{\infty} t^{s-1} e^{-t} dt$, we can easily represent D_3 as follows:

$$D_3 = d_{sp}^{\alpha} \Big(\frac{I}{d_{sr}^{\alpha}\varepsilon\sigma^2 + d_{sp}^{\alpha} I}\Big)^{m+1} \Gamma(m+1, \frac{d_{sr}^{\alpha}\varepsilon\sigma^2 + d_{sp}^{\alpha} I}{\rho\sigma^2})$$
$$\approx \Gamma(m+1, k). \quad (50)$$

Let $s = \frac{d_{sr}^{\alpha}\varepsilon\sigma^2 + d_{sp}^{\alpha} I}{I} y$, D_4 can be expressed by:

$$D_4 = d_{sp}^{\alpha} \ln(\frac{I}{d_{sr}^{\alpha}\varepsilon\sigma^2 + d_{sp}^{\alpha} I}) \Big(\frac{I}{d_{sr}^{\alpha}\varepsilon\sigma^2 + d_{sp}^{\alpha} I}\Big)^{m+1}$$
$$\times \underbrace{\int_{\frac{d_{sr}^{\alpha}\varepsilon\sigma^2 + d_{sp}^{\alpha} I}{\rho\sigma^2}}^{\infty} e^{-s} s^m \ln(s) ds}_{D_5}. \quad (51)$$

D_5 can be evaluated by applying integration by parts and mathematical induction as:

$$D_5 = \ln(\frac{a_1 + a_2 I}{\rho}) e^{-\frac{a_1 + a_2 I}{\rho}} \sum_{i=0}^{m} \frac{m!}{(m-1)!} (\frac{a_1 + a_2 I}{\rho})^{m-i}$$
$$+ \sum_{i=0}^{m-1} \frac{m!}{(m-i)!} \Gamma(m-i, \frac{a_1 + a_2 I}{\rho}) + E_1(\frac{a_1 + a_2 I}{\rho}), \quad (52)$$

where $E_1(x)$ is exponential integral function [21], $a_1 = d_{sr}^{\alpha}\varepsilon$, $a_2 = \frac{d_{sp}^{\alpha}}{\sigma^2}$.

D_5 can be approximated as a constant, when $I \to \infty$:

$$D_5 \approx \ln(a_2 k) e^{-a_2 k} \sum_{i=0}^{m} \frac{m!(a_2 k)^{m-i}}{(m-1)!} + E_1(a_2 k)$$
$$+ \sum_{i=0}^{m-1} \frac{m! \Gamma(m-i, a_2 k)}{(m-i)!}. \quad (53)$$

Based on (48), (50), (51) and (53), the third part C can be approximated as follows:

$$C \approx e^{-\frac{k d_{sp}^{\alpha}}{\sigma^2}} (1 - \frac{d_{sr}^{\alpha}\varepsilon}{\rho}). \quad (54)$$

Substituting (41), (44), (54) into (36), the proof is completed.

REFERENCES

[1] Z. Ding, X. Lei, G. K. Karagiannidis, R. Schober, J. Yuan, and V. Bhargava, "A survey on non-orthogonal multiple access for 5G networks: Research challenges and future trends," *IEEE J. Sel. Areas Commun.*, vol. 35, no. 10, pp. 2181–2195, Oct. 2017.
[2] S. M. R. Islam, N. Avazov, O. A. Dobre, and K.-S. Kwak, "Power-domain non-orthogonal multiple access (NOMA) in 5G systems: Potentials and challenges," *IEEE Commun. Surveys Tuts.*, vol. 19, no. 2, pp. 721–742, 2nd Quart., 2017.
[3] L. Dai, B. Wang, Z. Ding, Z. Wang, S. Chen, and L. Hanzo, "A survey of non-orthogonal multiple access for 5G," *IEEE Commun. Surveys Tuts.*, vol. 20, no. 3, pp. 2294–2323, 3rd Quart., 2018.
[4] *Study on Downlink Multiuser Superposition Transmission for LTE, TSG RAM Meeting 67*, document RP-150496, 3rd Generation Partnership Project (3GPP), Mar. 2018.
[5] Q. C. Li, H. Niu, A. T. Papathanassiou, and G. Wu, "5G network capacity: Key elements and technologies," *IEEE Veh. Technol. Mag.*, vol. 9, no. 1, pp. 71–78, Mar. 2014.
[6] Z. Ding, Z. Yang, P. Fan, and H. V. Poor, "On the performance of non-orthogonal multiple access in 5G systems with randomly deployed users," *IEEE Signal Process. Lett.*, vol. 21, no. 12, pp. 1501–1505, Dec. 2014.
[7] M. F. Kader and S. Y. Shin, "Coordinated direct and relay transmission using uplink NOMA," *IEEE Wireless Commun. Lett.*, vol. 7, no. 3, pp. 400–403, Jun. 2018.
[8] Z. Yang, Z. Ding, P. Fan, and N. Al-Dhahir, "A general power allocation scheme to guarantee quality of service in downlink and uplink NOMA systems," *IEEE Trans. Wireless Commun.*, vol. 15, no. 11, pp. 7244–7257, Nov. 2016.
[9] Z. Ding, M. Peng, and H. V. Poor, "Cooperative non-orthogonal multiple access in 5G systems," *IEEE Commun. Lett.*, vol. 19, no. 8, pp. 1462–1465, Aug. 2015.
[10] Z. Yang, Z. Ding, Y. Wu, and P. Fan, "Novel relay selection strategies for cooperative NOMA," *IEEE Trans. Veh. Technol.*, vol. 66, no. 11, pp. 10114–10123, Nov. 2017.
[11] P. Xu, Z. Yang, Z. Ding, and Z. Zhang, "Optimal relay selection schemes for cooperative NOMA," *IEEE Trans. Veh. Technol.*, vol. 67, no. 8, pp. 7851–7855, Aug. 2018.
[12] L. Lv, J. Chen, and Q. Ni, "Cooperative non-orthogonal multiple access in cognitive radio," *IEEE Commun. Lett.*, vol. 20, no. 10, pp. 2059–2062, Oct. 2016.
[13] Y. Liu, Z. Ding, M. Elkashlan, and J. Yuan, "Non-orthogonal multiple access in large-scale underlay cognitive radio networks," *IEEE Trans. Veh. Technol.*, vol. 65, no. 12, pp. 10152–10157, Dec. 2016.
[14] L. Lv, J. Chen, Q. Ni, and Z. Ding, "Design of cooperative non-orthogonal multicast cognitive multiple access for 5G systems: User scheduling and performance analysis," *IEEE Trans. Commun.*, vol. 65, no. 6, pp. 2641–2656, Jun. 2017.
[15] L. R. Varshney, "Transporting information and energy simultaneously," in *Proc. IEEE Int. Symp. Inf. Theory*, Jul. 2008, pp. 1612–1616.
[16] X. Zhou, R. Zhang, and C. K. Ho, "Wireless information and power transfer: Architecture design and rate-energy tradeoff," *IEEE Trans. Commun.*, vol. 61, no. 11, pp. 4754–4767, Nov. 2013.
[17] P. D. Diamantoulakis, K. N. Pappi, Z. Ding, and G. K. Karagiannidis, "Wireless-powered communications with non-orthogonal multiple access," *IEEE Trans. Wireless Commun.*, vol. 15, no. 12, pp. 8422–8436, Dec. 2016.
[18] Y. Liu, Z. Ding, M. Elkashlan, and H. V. Poor, "Cooperative non-orthogonal multiple access with simultaneous wireless information and power transfer," *IEEE J. Sel. Areas Commun.*, vol. 34, no. 4, pp. 938–953, Apr. 2016.
[19] Z. Yang, Z. Ding, P. Fan, and N. Al-Dhahir, "The impact of power allocation on cooperative non-orthogonal multiple access networks with SWIPT," *IEEE Trans. Wireless Commun.*, vol. 16, no. 7, pp. 4332–4343, Jul. 2017.
[20] J. Lee, H. Wang, J. G. Andrews, and D. Hong, "Outage probability of cognitive relay networks with interference constraints," *IEEE Trans. Wireless Commun.*, vol. 10, no. 2, pp. 390–395, Feb. 2011.
[21] I. S. Gradshteyn and I. M. Ryzhik, *Table of Integrals, Series, and Products*, 6th ed. New York, NY, USA: Academic, 2000.

YUEHAO YU received the B.S. degree in communication engineering from Shaoguan University, Shaoguan, China, in 2016. She is currently pursuing the M.S. degree with the College of Photonic and Electronic Engineering, Fujian Normal University. Her research interests include non-orthogonal multiple access, and cooperative and energy harvesting networks.

ZHENG YANG received the B.S. degree in mathematics from Minnan Normal University, Zhangzhou, in 2008, the M.S. degree in mathematics from Fujian Normal University, Fuzhou, China, in 2011, and the Ph.D. degree in information and communications engineering from Southwest Jiaotong University, Chengdu, China, in 2016. He was a Visiting Ph.D. Student with the School of Electrical and Electronic Engineering, Newcastle University, Newcastle upon Tyne, U.K., in 2014. He is currently an Associate Professor with the College of Photonic and Electronic Engineering, Fujian Normal University. His research interests include 5G networks, cooperative and energy harvesting networks, and signal design and coding. He received the Excellent Doctoral Thesis Award from the China Education Society of Electronics, in 2017, and the 2018 IEEE Signal Processing Society Best Signal Processing Letter Award.

YI WU received the B.Eng. degree in radio technology from Southeast University, Nanjing, China, in 1991, the M.S. degree in communications and information systems from Fuzhou University, Fuzhou, China, in 2004, and the Ph.D. degree in information and communication engineering from Southeast University, in 2013. She is currently a Professor with the College of Photonic and Electronic Engineering, Fujian Normal University. Her research interests include 5G networks, vehicular ad hoc networks, and communication protocols.

JAMAL AHMED HUSSEIN received the B.Sc. degree (Hons.) in electrical engineering from the Electrical Department, College of Engineering, University of Salahaddin, Erbil, Iraq, in 2001, the M.Sc. degree in electrical engineering from the Electrical Department, College of Engineering, University of Sulaimani, Sulaimani, Iraq, in 2007, and the Ph.D. degree in electrical and electronic engineering from Newcastle University, Newcastle Upon Tyne, England, U.K., in 2017.

He is currently a Senior Communication Engineer with the Directorate of Post and Communications, Sulaimaniyah, Ministry of Transportation and Communications—KRG, Iraq. His research interests include wireless communication, cooperative communication, cognitive radio, NOMA, 5G, and energy harvesting. He also acts as a Reviewer for several IEEE journals and the IET *Communications*.

WEN-KANG JIA received the Ph.D. degree from the Department of Computer Science, National Chiao Tung University (NCTU), Hsinchu, Taiwan, in 2011. He had been a Senior Engineer and Manager, since 1991, in various networking areas, including ICT manufacturer, network integrator, and telecomm service provider. He is currently a Professor with the College of Photonic and Electronic Engineering, Fujian Normal University. His recent research interests include the OSI layer-2 $\sim$ 5, such as TCP/IP protocols design, mobile management, error resilience coding, multimedia communications, NAT traversal, routing and switching, multicasting and broadcasting, teletrafic engineering, IP-optical convergence networks, P2P overlay networks, and wireless networks. He has published over 15 journal articles, over 30 international conference papers, three book chapters, and three patents. His work has been cited more than 300 times.

ZHICHENG DONG received the B.E., M.S., and Ph.D. degrees from the School of Information Science and Technology, Southwest Jiaotong University, Chengdu, China, in 2004, 2008, and 2016, respectively. From 2013 to 2014, he was a Visiting Scholar with the Department of Electrical and Computer Engineering, Utah State University, USA. From 2018 to 2019, he was a Research Fellow with the Department of Electrical and Computer Engineering, Columbia University, USA. Since 2019, he has been a Professor with the School of Engineering, Tibet University, Lhasa, China. His research interests include artificial intelligence, computer vision, adaptation technology, performance analysis, and signal processing for high mobility wireless communications. He served as a TPC member for major international conferences, such as IEEE ICC, IEEE GLOBECOM, IEEE WCNC, IEEE VTC, and IEEE PIMRC. He also served as a Reviewer for many well-known journals, such as the IEEE *Wireless Communications Magazine*, the IEEE JOURNAL ON SELECTED AREAS IN COMMUNICATIONS, and the IEEE TRANSACTIONS ON VEHICULAR TECHNOLOGY.